

Energy comparative analysis of MPPT techniques for PV system using interleaved soft-switching boost converter

M. Muthuramalingam¹, P. S. Manoharan^{2*}

¹ P.T.R. College of Engineering and Technology, Madurai, Tamilnadu, India

² Thiagarajar College of Engineering, Madurai, Tamilnadu, India

(Received September 1 2014, Accepted December 29 2014)

Abstract. The availability of solar energy varies widely with ambient temperature and different atmospheric conditions and hence the maximum power point (MPP) of photovoltaic system (PV) system is not stable. Therefore, a maximum power point tracking (MPPT) controllers are needed to operate the PV at its MPP. This work presents an evaluation of four different MPPT techniques for PV system such as perturb and observation (P&O), incremental conductance (INC), fuzzy logic controller (FLC), and genetic algorithm (GA). These MPPT techniques are implemented in an interleaved soft switching boosts converter (ISSBC) and performance comparison is made for these four MPPT algorithms in terms of parameters like global peak, tracking speed and power extraction. These algorithms are methodically investigated by means of simulation and a projected efficiency estimate method of experimentation. The simulation and hardware results show that GA algorithm is outperforming than the other algorithms.

Keywords: maximum power point tracking (MPPT), fuzzy logic controller (FLC), genetic algorithm (GA), microcontroller, interleaved soft switching boost inverter (ISSBC)

1 Introduction

Photovoltaic energy has increased interest in electrical power applications, since it is considered as a basically limitless and generally on hand energy resource. However, the output power induced in the photovoltaic modules depends on solar irradiance and temperature of the solar cells. This makes the extraction of maximum power a complex task. The efficiency of the PV generation depends on maximum power extraction of PV system. Therefore, to maximize the efficiency of the renewable energy system, it is necessary to track the maximum power point of the PV array^[19]. The PV array has a single in service point that can supply maximum power to the load. This point is called the maximum power point (MPP). The locus of this point has a nonlinear distinction with solar irradiance and the cell temperature. Thus, in order to operate the PV array at its MPP, the PV system must contain a maximum power point tracking (MPPT) controller. Many MPPT techniques have been reported in the literature. The P&O method is an iterative algorithm to track the MPP by measuring the current and voltage of the PV module. This algorithm is easy to implement but the problem of oscillation of operating point around MPP is unavoidable as discussed in [9, 10]. INC method presented in [7, 11] is most widely used method. It tracks the MPP by comparing instantaneous conductance to the incremental conductance. The INC method requires complex computations to acquire good accuracy under rapidly changing weather conditions and the response time to reach MPP is also relatively long as discussed in [2, 13]. The Perturbation and Observation (P&O) and Incremental conductance (INC) algorithms, which works satisfactorily when the irradiance varies very slowly but fails to track global MPP when irradiance changed. The above mentioned algorithms work satisfactorily only under uniform irradiance conditions in which PV curve has a unique MPP. Recently artificial intelligence methods which include Fuzzy and Neural Network

* Corresponding author. E-mail address: psmeee@tce.edu.

have been applied to track. The fuzzy logic controllers have the advantages of robustness, simplicity in design and it does not need accurate mathematical model. The selection of parameters and membership function in fuzzy logic is not easy as it needs expert knowledge and experimentation as discussed in [4, 15–18]. Artificial neural network (ANN) based alleviate the problem of oscillation around MPP and there is no need for the prior knowledge of the PV parameters^[3, 6, 12, 20]. The dataset for the ANN is obtained from experimental measurements. Adaptive neuro fuzzy inference system (ANFIS) based MPPT are presented in [1, 8, 14]. The AI based MPPT are effective but the computational cost is high and tracking speed is low. Hence optimization techniques such as GA and Particle swarm optimization (PSO) are used to track MPP. The MPPT techniques are implemented in ISSBC. The ISSBC converter exhibits soft switching characteristics as discussed in [5]. The objective of this paper is to analyze different MPPT algorithms: P&O, INC, FLC and GA being used to extract the maximum DC power from PV module various isolation and cell temperature. The functional block diagram as shown in Fig. 1, Matlab simulation results are validated by experimentally using 16F877A microcontroller platform.

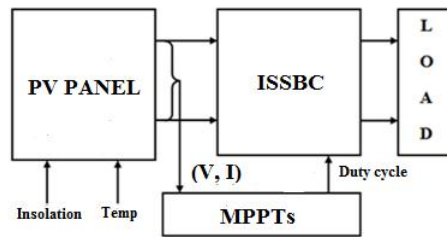


Fig. 1. General Diagram of load connected photovoltaic system

2 PV array modeling and simulation

The PV array used in the proposed system is 72 multi-crystalline silicon solar cells in series able to provide 150W of maximum power PV module and it is simulated as per datasheet In this model, a PV cell is represented by a current source in parallel with a diode and a series resistance, the basic current equation is given in Eq. (1).

$$I = I_{pv,cell} - I_{0,cell} \left[\exp \frac{qv}{akT} - 1 \right], \quad (1)$$

where $I_{pv,cell}$ is current generated by the incident light (directly proportional to sun irradiation), $I_{0,cell}$ is leakage current of the diode, q is electron charge $1.6021e10 - 19 C$, k is Boltzmann constant, T is temperature of the PN junction, α is Diode ideality constant. To develop embedded simulink model based on current equation and manufacturer's data sheet as per parameter of BP SX 150S model.

3 MPPT control algorithms

In order that the power transferred from the source to the load is maximized, according to the maximum power transfer theorem, it is essential that the source impedance is identical to the load impedance. The problem PV array impedance varies with respect to climate conditions like solar insolation and temperature. Thus MPPT is nothing but a tractable impedance matching scheme, which as a result leads to maximum power transfer.

3.1 P&O algorithm

The P&O algorithm has the advantage of simple software and hardware credit. The P&O algorithm perturbs the duty cycle which controls the power converter. The algorithm uses voltage and current measurements

to calculate change in power over a change in time (ΔP) and change in the duty cycle (ΔD) of the signal sent to the gate of the switch in the converter. Given that ΔP and ΔD can be each whichever positive or negative, there are four cases to resolve whether the duty cycle of the gate signal should be increased or decreased. The flowchart in Fig. 2 clearly explains the P&O algorithm.

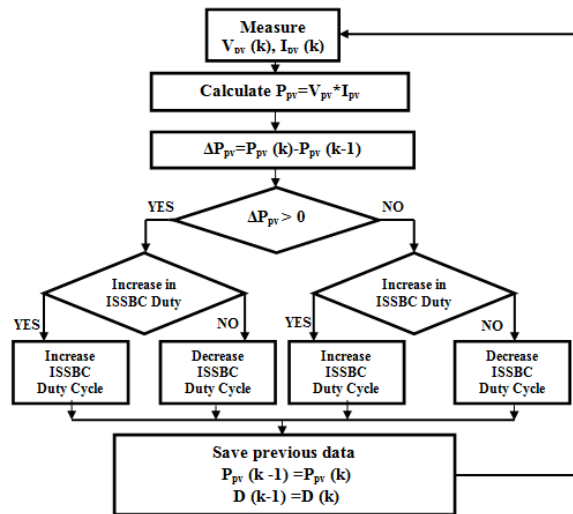


Fig. 2. P&O algorithm

3.2 Incremental conductance

Another commonly cited MPPT algorithm is the incremental conductance (INC) algorithm. This scheme tracks the maximum power point by comparing the solar array incremental and instantaneous conductance, the function of this procedure is explained in the flowchart in Fig. 3. The PV panel voltage and current are measured at fixed sampling intervals and fed to the controller to calculate the PV panel power. The PV panel incremental conductance is predictable by measuring miniature changes in array voltage and current. The PV panel instant conductance is calculated by dividing the array current by the voltage. Once these variables are updated, the method tracks the maximum power point by comparing the incremental and instant conductance of the solar array until the maximum power point (MPP) is reached, as illustrated in Fig. 3. In conclusion, the null value of the slope of the PV array power versus voltage curve infrequently occurs.

3.3 Fuzzy logic controller

Conventional methods of tracking the most favorable point of operation have shown their restrictions to sudden changes of climate and the load associated to the panel. Another encouraging tracker algorithm is fuzzy logic. The operation of this technique is explained in the block diagram shown in Fig. 4. In this paper the fuzzy inference rule is carried out by using Mamdani’s method and the defuzzification use the centre of gravity to compute the output of this FLC which is the duty cycle. FLC system has two inputs and one output. The two FLC input variables are the error $E(k)$ and change of error $\Delta E(k)$ at sampled times k defined. Where $P(k)$ and $V(k)$ are the instant power and voltage of the photovoltaic system respectively $E(k)$ is zero at the maximum power point of PV array.

The input $E(k)$ shows if the operation point at the instant k is located on the left or on the right of the MPPT on the PV Characteristic while the input $\Delta E(k)$ expresses the moving direction of this point. The objective of designed FLC is to track maximum power irrespective of panel voltage variations. Accordingly FLC uses two input variables: change in PV array Power (ΔP_{in}) and change in PV array voltage (ΔV_{in}) corresponding to the two sampling time instants and determining duty cycle of converter.

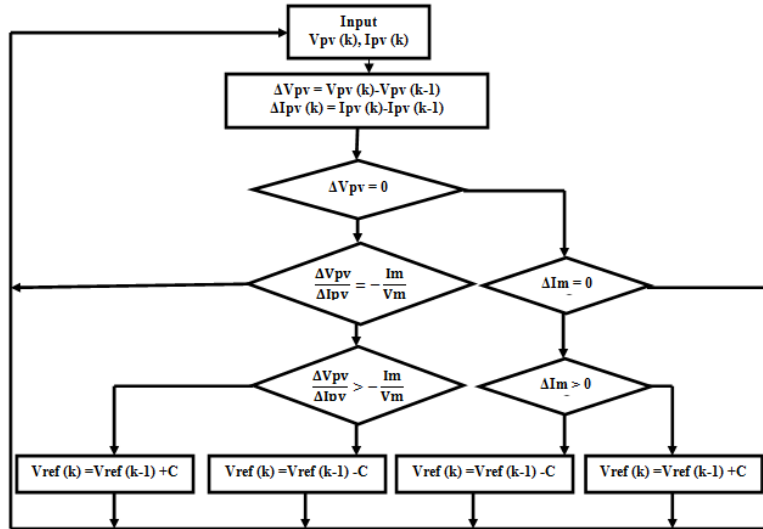


Fig. 3. Incremental conductance algorithm

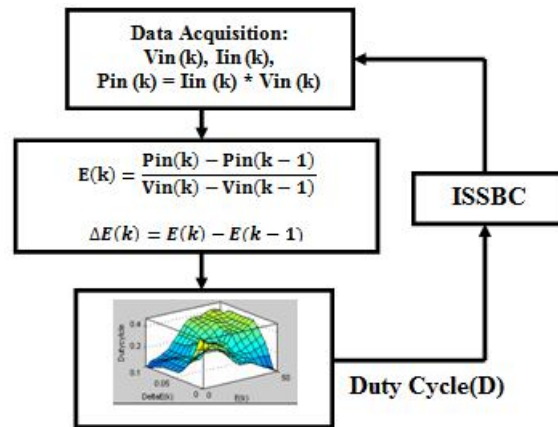


Fig. 4. Fuzzy logic systems

3.4 Genetic algorithm

The MPPT algorithm based on GA Genetic Algorithm (GA) is an optimization system that resembles natural genetics. Using this method, an optimal set of parameters is resolute based on a “survival of the fittest” principle. In fact, there are three basic operators concerned in the look for procedure of a GA: selection, crossover, and mutation. Selection is a method which chooses a genetic material from the current generation’s population for enclosure in the next generation’s population according to their fitness. Crossover operator combines two chromosomes to produce a new genetic material . Mutation operator maintains genetic diversity from one generation of population to the next and aims to achieve some stochastic dissimilarity of GA in order to get an earlier convergence to solve this problem customized the algorithm by resetting the first population whenever it detects a variation of irradiance and cell temperature. Accordingly, the GA is reinitialized every time the following two conditions are satisfied as given in Eq. (2) and Eq. (3).

$$|V(k + 1) - V(K)| < \Delta V, \tag{2}$$

$$\left| \frac{P_{pv}(k + 1) - P_{pv}(k)}{P_{pv}(k)} \right| > \Delta P. \tag{3}$$

The chromosomes position corresponds to the desired output voltage at iteration (k). The initial population that is composed by chromosomes parents includes four individuals which are applied successively. The initial

positions of this population are given by Eq. (4).

$$[P1, P2, P3, P4] = [0.8, 0.6, 0.4, 0.2] V_{oc}. \quad (4)$$

The fitness is the generated power P_{pv} , it is sorted decreasingly, and the criterion of selection is performed by elitism. The crossover step consists of combining two chromosomes parents to produce a child. In fact, this step is based on Eq. (5) and Eq. (6).

$$\text{child}(k) = r.P(r) - (1 - r).P(k + 1), \quad (5)$$

$$\text{child}(k + 1) = (r - 1).P(k) - (r).P(k + 1), \quad (6)$$

where, r is a random number $r \in [0, 1]$. The relation between the output voltage and the duty cycle of the ISSBC is written as Eq. (7).

$$a(k) = \text{child}(k)/V_{oc}. \quad (7)$$

In this work, we do not take into account the step of mutation regardless its impact on the convergence of the dynamic response and the apparition of oscillations, and this is due to the sequential aspect of chromosomes. Based on the GA equation Matlab programmed and embedded in user interface function, initialized in simulation system.

4 Soft switching boost converter

The interleaved boost inverter consists of two single-phase boost inverters that are linked in parallel and inverters operating 180 degrees out of phase with 30 kHz switching frequency. Interleaved converter mode 60 kHz effect is achieved by phase shifting of the two 30 kHz switching signals^[5, 14]. Because the inductor ripple currents are out of phase, they cancel each other and the input-ripple current reduce to 12% of that of a conventional boost inverter. The best input-inductor-ripple-current deletion occurs at 50% duty cycle. Therefore, the interleaved inverters have the wider continuous current mode, the condensed input current ripple and output voltage ripple, and lower switching losses, therefore the output voltage of the solar cell can be boosted with high effectiveness.

5 Simulation validation

The PV module parameters are obtained from the 150 Watts Multicrystalline PV Module technical datasheet. All algorithm tests were performed considering the same temperature and irradiation steps. Such parameters are considered at the Standard Test Condition (STC): 1000 W/m² and cell temperature of 25 °C. The simulation diagram as shown in Fig. 5, first the characteristics of the PV module are validated and connected with ISSBC then the performance of the MPPT techniques under various conditions is evaluated to investigate the output power efficiency. The simulation validation of PV module and converter results of the I-V and P-V characteristics of PV module as a function of irradiation and temperature shown in Figs. 6 and 7. It can be observed quite similar to the 150 watts PV module as per data sheet. The sampling time considered is equal to 0.02s, and the switching frequency is chosen equal to the 30 kHz.

5.1 Slowly variation with ripple irradiation

In view of a real condition, the solar irradiance varies from a certain minimum value to the maximum value and then goes down to a different minimum value. A parallel pattern is also appropriate for the PV cell temperature. To simulate a real time situation, the solar irradiance and temperature is different consequently as shown in Fig. 8. The solar irradiance is varied from nearly 200 to 1000 W/m² with a peak value of 1000 W/m² and with a 4% ripple. The temperature is varied from 15 °C to 55 °C and back to 15 °C. Tabulated the detail of the response time, output voltage, duty cycle, efficiency and power. From the Tab. 1, the efficiency is about 97-98% for all MPPT algorithms, but the GA is the most efficiency and converges quickly to the global MPP.

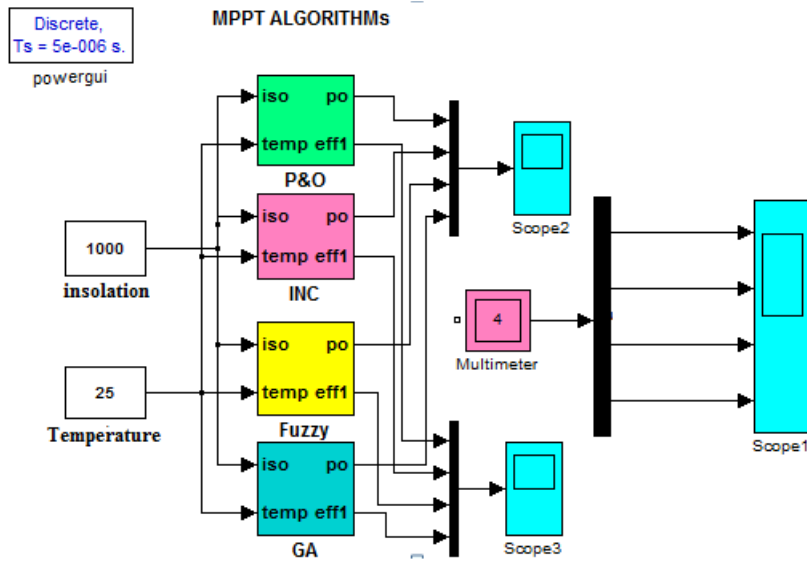


Fig. 5. Simulation system

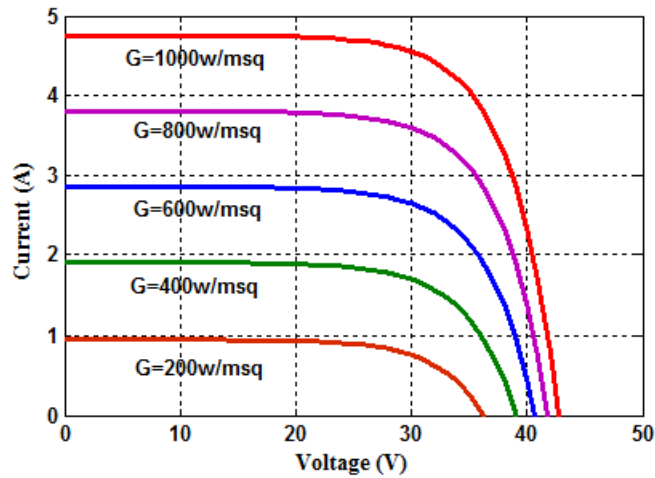


Fig. 6. I-V Curve solar radiation

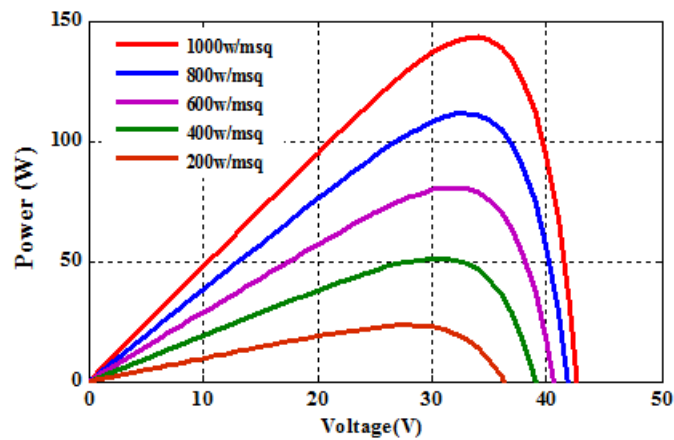


Fig. 7. P-V Curve

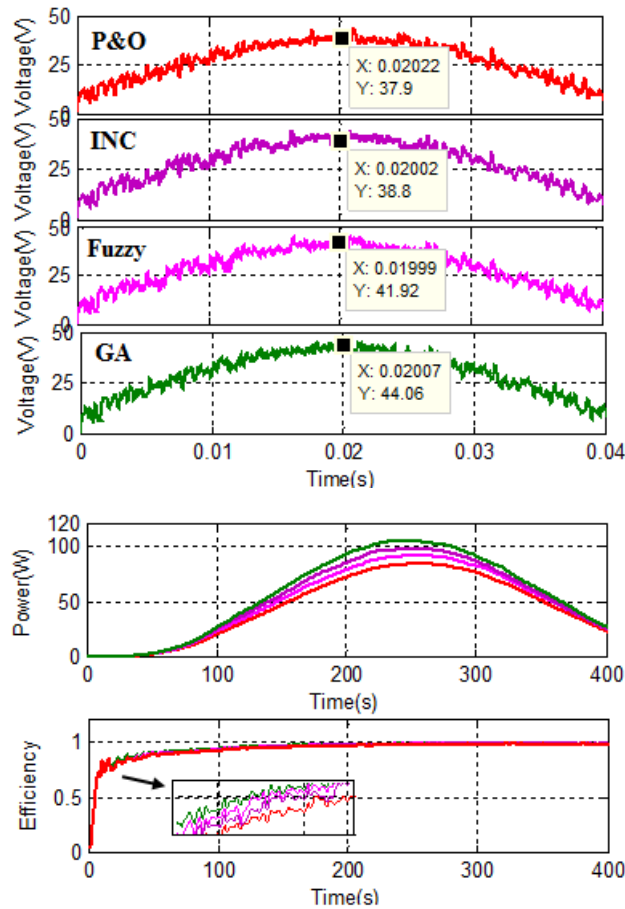


Fig. 8. Simulation of slowly changing irradiance corresponding MPPT algorithm output voltage, output power and efficiency

Table 1. Simulation of slowly changing irradiance corresponding MPPT algorithm output voltage, output power and efficiency

MPPT algorithm	Voltage Range (V_{dc})	Power Range (W_{dc})	Efficiency range (%)	Duty cycle Range (MI)	Response time range (ms)
GA	12.27-44.06	29.98-103.90	0.97-0.98	0.21-0.23	7-10
Fuzzy	11.03-41.92	28.64-96.52	0.95-0.97	0.19-0.21	8-11
INC	11.03-38.23	27.64-90.38	0.94-0.97	0.17-0.21	10-15
P&O	10.38-37.9	26.08-83.77	0.94-965	0.16-0.20	12-16

5.2 Dynamic varying the solar radiation

Simulations are carried out of five techniques under dynamically changes solar irradiances at temperature of 25 °C. Fig. 9 shows output voltage of sudden changes in solar irradiation from 600 to 1000 W/m^2 . The detailed dynamic configuration pattern and correspond PV output result parameter tabulated in Tabs. 2 and 3 respectively. In this analysis the five techniques are able to extract the MPP. The power delivered by P&O and incremental conductance power outputs 48.80 and 54.08 watts respectively 600 W/m^2 but P&O oscillation around MPP, both controllers does not exceed global maximum power. Fuzzy power equal to 59.03 at 600 W/m^2 , all algorithms oscillation to reach new MPP sudden change in irradiation. The GA power extracted 62.28 *watts* at 600 W/m^2 fast response to reach the new MPP after solar irradiation changes. Higher power extracted from GA controller compare to all other controllers.

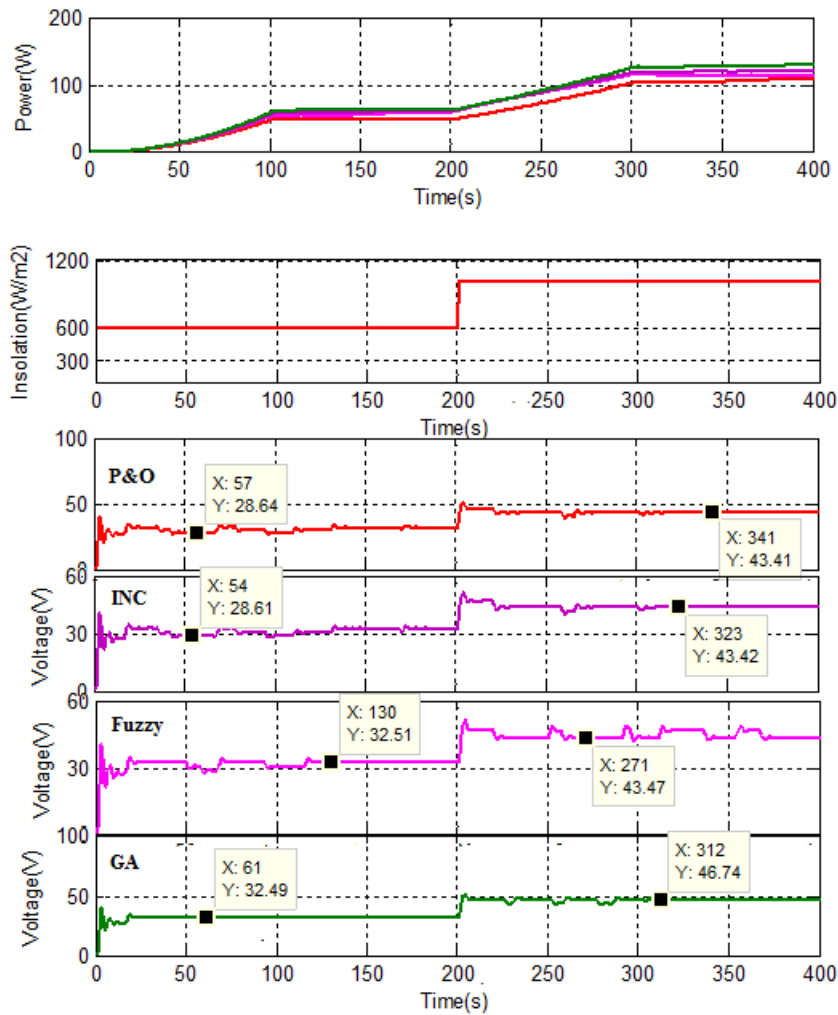


Fig. 9. Dynamic variation of irradiation

Table 2. Dynamic response patterns

Pattern	Irradiation (W/m^2) (from $t = 0s$ to $t = 200s$)	(from $t = 200s$ to $t = 400s$)	Cell Temperature ($^{\circ}C$)
SD1	600	1000	25

Table 3. Dynamic response of simulation

MPPT	Pattern	Simulation time configuration							
		From $t = 0s$ to $t = 200s$			From $t = 200s$ to $t = 400s$			Response Time (s)	Efficiency (%)
V_{dc}	P_{dc}	MI	V_{dc}	P_{dc}	MI				
P&O	SD1	28.64	48.8	0.21	43.41	103.1	0.22	0.0037	0.965
INC	SD1	28.81	54.08	0.22	43.42	113.3	0.215	0.0029	0.97
Fuzzy	SD1	32.51	59.08	0.22	43.47	119.5	0.22	0.0028	0.98
GA	SD1	32.49	62.28	0.23	46.74	126.5	0.23	0.0013	0.985

6 Experimental validation

The simulation results are verified experimentally using 16F877A microcontroller. The ISSB converter, 16F877A microcontroller, serial port MA232, digital oscilloscope and rheostat is used as DC resistive load. The P&O, IC, Fuzzy, and GA techniques microcontroller program is developed to track the MPPT. The proposed system is tested in laboratory and the photograph of the experimental setup that includes the 16F877A microcontroller is shown in Fig. 10. The solar panel is not shown in photograph. The switching frequency

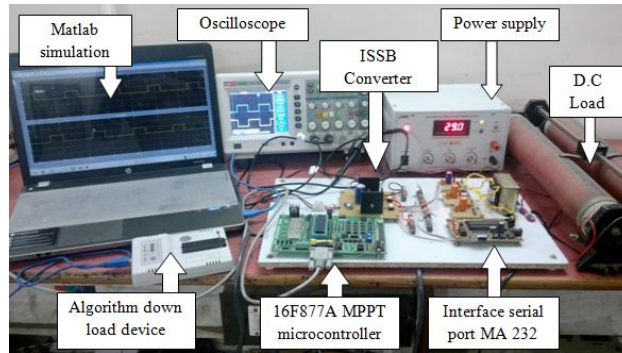


Fig. 10. Experimental system

of ISSBC is 30 kHz . The controller program are scaled down and fusing into 16F877A microcontroller and generate gating signals to the ISSB converter. The MPPTs algorithm extracted power can be observed an ex- position of approximately 04:00 hrs range from 09:00 hrs to 14:00 hrs with different PV insolation and cell temperature. Actually, experiment measurement obtained from different MPPT algorithm conducted on six different sunny days.

The availed insolation, temperature and different climate pattern for experimental condition is tabulated in Tab. 4 at consign intervals of time; observe the output power as shown in Tab. 5. The output power values of P&O, IC, Fuzzy, and GA are 106.80, 108.40, 107.80, and 116.60 watts at case 7, corresponding energy comparison bar chart as shown in Fig. 11. From observed experimental result tabulation GA algorithm ex- tract global maximum power recovery especially when solar panel different irradiation. In addition, the GA algorithm less transient, quick steady state response and efficiency compare to the rest of all other algorithm.

Table 4. Pattern of experimental result

Pattern	Time of day	Insulation (W/m^2)	Temperature ($^{\circ}C$)
case 1	8.3	300	37.3
case 2	16.3	400	36.7
case 3	14.35	730	36
case 4	11	800	41
case 5	11.15	860	36
case 6	12	950	44
case 7	13	1040	44

Table 5. Experimental output power of MPPTs algorithm

Pattern	P&O	INC	Fuzzy	GA
case 1	13.34	11.53	13.15	14.19
case 2	24.49	24.86	25.01	26.04
case 3	79.25	80.5	80.25	84.27
case 4	89.3	90	90.3	97.96
case 5	96.75	98.21	96.75	102.9
case 6	100.5	102.1	102.9	106.9
case 7	106.8	108.4	107.8	113.6

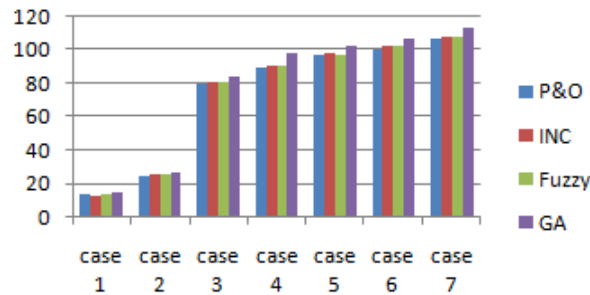


Fig. 11. Energy comparison chart

7 Conclusion

This paper analyzes the performance of P&O, IC, Fuzzy, and GA algorithms implemented in ISSBC for PV systems. The configuration for the proposed system is designed and simulated using MATLAB/simulink and implemented in 16F877A microcontroller. The proposed GA algorithm shows good dynamic performance to track the MPP of the PV even under the rapid change of the irradiation and cell temperature. The ISSBC converter can be more efficient than the conventional converter; simple hardware design gives maximum efficiency at full load condition. The ISSBC with GA can provide the overall efficiency of about 98% which is higher than other algorithms due to decreasing the frequency of operation and switching losses and the response time is also less as compared to other algorithms. The results obtained are encouraged to use the ISSBC with GA in applications such as PV generation system.

References

- [1] A. Mellit, S. Kalogeria. ANFIS-based modeling for photovoltaic power supply system. *Renewable Energy*, 2011, **36**(1): 250–255.
- [2] A. Mohammedi, N. Mezzai, et al. Impact of shadow on the performances of a domestic photovoltaic pumping system incorporating an MPPT control: A case study in Bejaia, North Algeria. *Energy Conversion and Management*, 2014, **6**(84): 20–29.
- [3] A. Ravi, P. Manoharan, et al. Harmonic reduction of three-phase multilevel inverter for grid connected photovoltaic system using closed loop switching control. *International review on Modeling and Simulation*, 2012, **5**(5): 1934–1942.
- [4] C. Salah, M. Ouali. Comparison of fuzzy logic and neural network in maximum power point tracker for PV systems. *Electric Power Systems Research*, 2011, **81**(1): 43–50.
- [5] D. Jung, Y. Ji, et al. Interleaved soft-switching boost inverter for photovoltaic power-generation system. *IEEE Transactions on Power Electronics*, 2011, **26**(4): 1137–1145.
- [6] F. Chekired, A. Mellit, et al. Intelligent maximum power point trackers for photovoltaic applications using FPGA chip: A comparative study. *Solar Energy*, 2014, **101**: 83–99.
- [7] K. Ishaque, Z. Salam, G. Lauss. The performance of perturb and observe and incremental conductance maximum power point tracking method under dynamic weather conditions. *Applied Energy*, 2014, **119**: 228–236.
- [8] K. Ravinder, M. Ansari, S. Shimi. Design and implementation of ANFIS based MPPT scheme with open loop boost converter for solar PV module. *International Journal of Advanced Research in Electrical and Electronics and Instrumentation Engineering*, 2014, pp 6517–6524.
- [9] K. Tey, S. Mekhilef. Modified incremental conductance MPPT algorithm to mitigate inaccurate responses under fast-changing solar irradiation level. *Solar Energy*, 2014, **101**: 333–342.
- [10] M. Aureliano, L. Galotto, L. Poltroonery. Evaluation of the main MPPT techniques for photovoltaic applications. *IEEE Transactions on Industrial Electronics*, 2013, **60**(3): 1156–1167.
- [11] M. Mahmud, H. Pota, M. Hossain. Nonlinear current control scheme for a single-phase grid-connected photovoltaic system. *IEEE Transactions on Sustainable Energy*, 2014, **5**(1): 218–227.
- [12] M. Muthuramalingam, P. Manoharan. Simulation and experimental validation of distributed MPPT algorithms for partially shaded photovoltaic systems. *Przeglad Elektrotechniczny*, 2014, pp 90–96.
- [13] M. Muthuramalingam, P. Manoharan. Simulation and experimental verification of mppt algorithms for partially shaded stand alone photovoltaic systems. *Power Electronics and Renewable Energy Systems*, 2015, pp 153–161.

- [14] M. Muthuramalingama, P. Manohara. Comparative analysis of distributed MPPT controllers for partially shaded stand alone photovoltaic systems. *Energy Conversion and Management*, 2014, **86**: 286–299.
- [15] M. Salhi, R. El-Bachtri. Maximum power point tracker using fuzzy control for photovoltaic system. *International Journal of Research and Reviews in Electrical and Computer Engineering*, 2011, **1**(2): 2046–2051.
- [16] N. Altin, S. Ozdemir. Three-phase three-level grid interactive inverter with fuzzy logic based maximum power point tracking controller. *Energy Conversion and Management*, 2013, **69**: 17–26.
- [17] N. Bader, H. Khaled, et al. Fuzzy logic control approach of a modified hill climbing method for maximum power point in microgrid standalone photovoltaic system. *IEEE Transactions on Power Electronics*, 2011, **26**: 1022–1030.
- [18] S. Arumugam, M. Thathan. Combined effect of fuzzy logic controller and optimized voltage vector in torque ripple reduction of direct torque controlled permanent magnet synchronous motor. *World Journal of Modeling and Simulation*, 2014, pp 92–107.
- [19] X. Gao, S. Li, R. Gong. Maximum power point tracking control strategies with variable weather parameters for photovoltaic generation systems. *Solar Energy*, 2013, **93**: 357–367.
- [20] Y. Liu, C. Liu, et al. Neural-network-based maximum power point tracking methods for photovoltaic systems operating under fast changing environments. *Solar Energy*, 2013, **89**: 42–53.